Protection against malaria in mice is induced by blood stage–arresting *histamine-releasing factor* (*HRF*)–deficient parasites

Claudia Demarta-Gatsi,[1] Leanna Smith,[1] Sabine Thiberge,[2] Roger Peronet,[1] Pierre-Henri Commere,[3] Mariette Matondo,[4] Lionel Apetoh,[6] Pierre Bruhns,[5] Robert Ménard,[2] and Salaheddine Mécheri[1]

[1]Unité de Biologie des Interactions Hôte Parasites, Centre National de la Recherche Scientifique ERL9195, Institut National de la Santé et de la Recherche Médicale U1201, [2]Unité de Biologie et Génétique du Paludisme, [3]Imagopole, [4]Spectrométrie de Masse Structurale et Protéomique, and [5]Anticorps en Thérapie et Pathologie, Institut National de la Santé et de la Recherche Médicale U1222, Institut Pasteur, F-75015 Paris, France
[6]Institut National de la Santé et de la Recherche Médicale U866, Université Bourgogne Franche-Comté et Centre Georges François Leclerc, 21000 Dijon, France

Although most vaccines against blood stage malaria in development today use subunit preparations, live attenuated parasites confer significantly broader and more lasting protection. In recent years, *Plasmodium* genetically attenuated parasites (GAPs) have been generated in rodent models that cause self-resolving blood stage infections and induce strong protection. All such GAPs generated so far bear mutations in housekeeping genes important for parasite development in red blood cells. In this study, using a *Plasmodium berghei* model compatible with tracking anti–blood stage immune responses over time, we report a novel blood stage GAP that lacks a secreted factor related to histamine-releasing factor (HRF). Lack of HRF causes an IL-6 increase, which boosts T and B cell responses to resolve infection and leave a cross-stage, cross-species, and lasting immunity. Mutant-induced protection involves a combination of antiparasite IgG2c antibodies and FcγR$^+$ CD11b$^+$ cell phagocytes, especially neutrophils, which are sufficient to confer protection. This immune-boosting GAP highlights an important role of opsonized parasite-mediated phagocytosis, which may be central to protection induced by all self-resolving blood stage GAP infections.

The Journal of Experimental Medicine

Live attenuated parasites, in particular genetically attenuated parasites (GAPs), are increasingly being considered as vaccines against malaria. Preerythrocytic GAPs fail to develop in the liver, whereas blood stage GAPs cause abortive infections in the blood. In both cases, GAP infection induces solid protection against challenge.

The notion that attenuated blood stage parasites can confer protection originated in early studies using irradiated parasites (Waki et al., 1982; Miyagami et al., 1987). More recently, it was found that infecting individuals with low doses of *Plasmodium falciparum*–infected RBCs (iRBCs) followed by rapid curative treatment induced strong cell-mediated immunity and durable protection against challenge (Pombo et al., 2002). Subsequently, blood stage GAPs were generated in rodent parasites, targeting genes involved in the purine salvage pathway in *Plasmodium yoelii* (Ting et al., 2008; Aly et al., 2010) or genes encoding a protease involved in hemoglobin degradation (Spaccapelo et al., 2010) and a merozoite surface protein involved in adhesion to RBCs (Spaccapelo et al., 2011) in *Plasmodium berghei*. These GAPs multiply suboptimally in the blood and cause infections that eventually self-resolve. Notably, abortive GAP-induced infections confer lasting protection against challenge with blood stages or mosquito transmission stages and depend on both cellular and humoral immunity (Ting et al., 2008; Aly et al., 2010).

Recently, we described the crucial role of histamine-releasing factor (HRF), also known as translationally controlled tumor protein, during development of *P. berghei* ANKA (*Pb*ANKA) in the host liver (Mathieu et al., 2015). In vivo development of *HRF*-deficient *Pb*ANKA parasites is severely impaired in the liver, caused by elevated levels of IL-6 (Pied et al., 1991). To test whether HRF might also modulate blood stage multiplication, we deleted the *HRF*-encoding gene in *P. berghei* NK65 (*Pb*NK65). *Pb*ANKA induces cerebral malaria in susceptible mice, with lesions starting at day 5 postinfection (p.i.) and mice dying from day 7–8 p.i. (Beghdadi et al., 2008), which precludes studies on adaptive immunity. In contrast, *Pb*NK65 does not cause cerebral malaria but hyperparasitemia, leading to mouse death by severe anemia around day 25 p.i. It thus provides an opportunity to track immune responses against blood stage parasites over a longer period of time.

RESULTS AND DISCUSSION

Deletion of the *hrf* gene in *Pb*NK65 parasites causes abortive blood stage development

We generated *hrf* knockout *Pb*NK65 parasites (*Pb*NK65-*hrfΔ*) by replacing the coding sequence of *pbhrf* (PBA

Correspondence to Salaheddine Mécheri: smecheri@pasteur.fr

Abbreviations used: APC, allo phyco cyanine; DTR, diphtheria toxin receptor; FA, formic acid; GAP, genetically attenuated parasite; gDNA, genomic DNA; hDHFR, human dihydrofolate reductase; HPRT, hypoxanthine phosphoribosyltransferase; HRF, histamine-releasing factor; iRBC, infected RBC; p.i., postinfection; qPCR, quantitative PCR; UTR, untranslated.

The Rockefeller University Press $30.00
J. Exp. Med. 2016 Vol. 213 No. 8 1419–1428
www.jem.org/cgi/doi/10.1084/jem.20151976

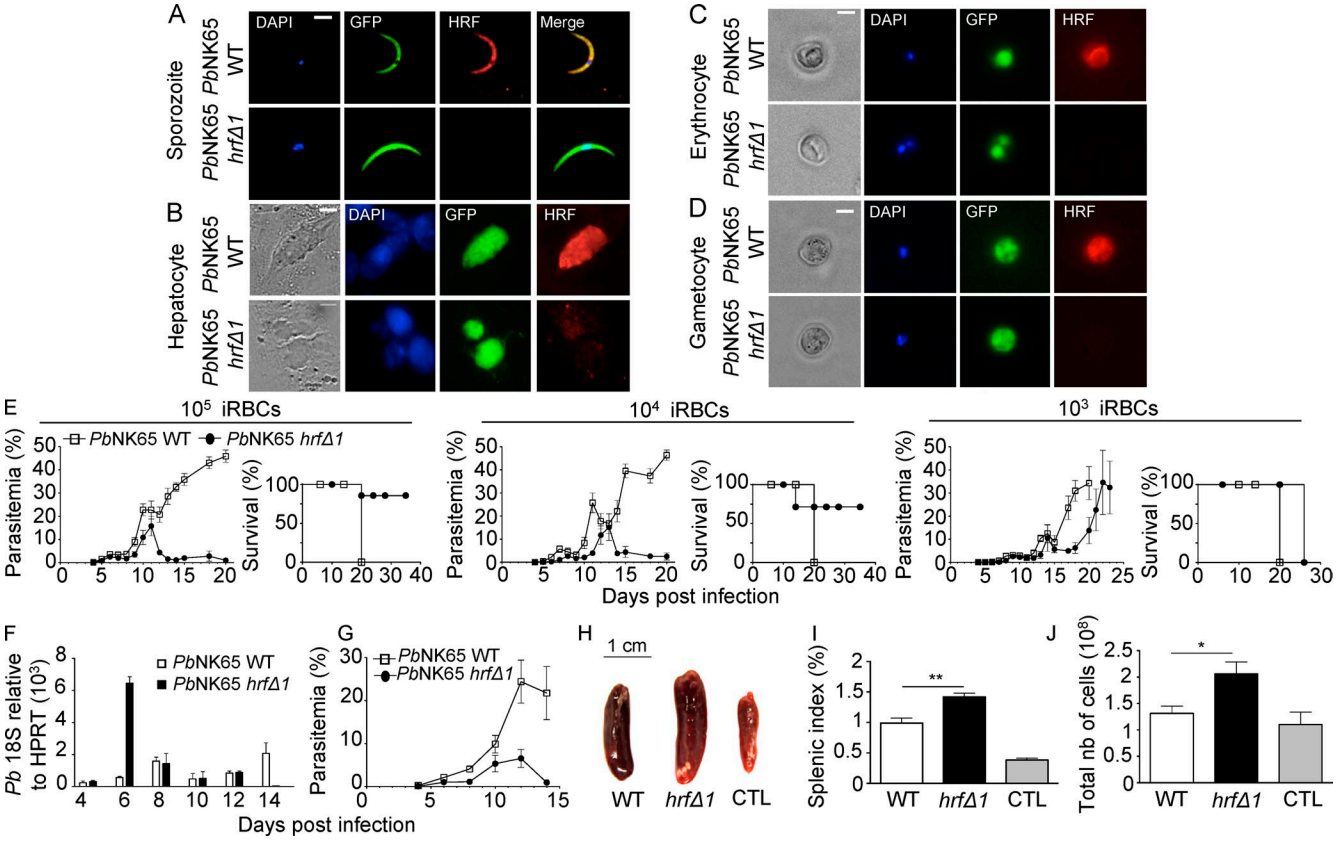

Figure 1. ***Pb*HRF protein expression and phenotype of mutant parasites.** (A–D) Anti-HRF–based immunofluorescence (red) was used to detect HRF in GFP-expressing WT or *Pb*NK65-*hrf*Δ1 sporozoites (A), liver stages obtained 48 h p.i. of HepG2 cells with sporozoites at a multiplicity of infection of 1:1 (B), infected erythrocytes (C), and gametocytes (D). Nuclear DNA stained with DAPI and phase-contrast images are shown. (A–D) Bars, 6 µm. (E) Blood stage parasitemia and survival of C57BL/6 mice (Kaplan-Meier survival plots) after i.p. injection of 10^5, 10^4, and 10^3 WT or *Pb*NK65-*hrf*Δ1–infected iRBCs measured over several days. (F and G) The kinetics of parasite load in the spleen of WT or *Pb*NK65-*hrf*Δ1–infected mice was determined by RT-qPCR analysis of *P. berghei* 18S rRNA expression relative to mouse HPRT mRNA levels (F) or flow cytometric analysis of parasitemia (G). (H) Spleen size of WT or *Pb*NK65-*hrf*Δ1–infected mice at day 6 p.i. (I and J) Splenic index (I) and total cell number (J) were compared at day 6 p.i. between mice infected with 10^5 WT and *Pb*NK65-*hrf*Δ1 iRBCs. Control: splenic index and cell number from naive mice. Error bars, SEM. Data are representative of three (A–D and H–J), six (E), and two (F and G) independent experiments with five to six mice per group. *, P = 0.029; **, P = 0.003; Mann-Whitney test. CTL, control; nb, number.

NKA_111050; UniProt accession no. A0A077XCV2) with the human dihydrofolate reductase (*hDHFR*)–selectable marker in a GFP-expressing *Pb*NK65 strain (Fig. S1 A). Two clones, *Pb*NK65-*hrf*Δ1 and 2, were selected from independent transfection experiments and verified to harbor the mutant locus by PCR (Fig. S1, B–D) and Southern blot analysis (Fig. S1 E). Using specific rabbit antibodies against recombinant *Pb*HRF (Mathieu et al., 2015), the protein was found to be expressed at all *Plasmodium* stages tested and to localize to the cytoplasm (Fig. 1, A–D), consistent with previous studies in human cells and *Pb*ANKA parasites (Bhisutthibhan et al., 1999; Mathieu et al., 2015). HRF was not detected in *Pb*NK65-*hrf*Δ1 parasites (Fig. 1, A–D), confirming both antibody specificity and successful gene knockout.

To assess the effect of *pbhrf* deletion on parasite blood stage development, C57BL/6 mice were infected i.p. with 10^5, 10^4, or 10^3 WT or *Pb*NK65-*hrf*Δ1–infected iRBCs, and parasite growth was monitored by flow cytometry. In mice infected with WT parasites, parasitemia increased steadily, resulting in severe malaria and death at approximately day 20 p.i. When using 10^5 or 10^4 infectious doses, *Pb*NK65-*hrf*Δ1 parasites multiplied like WT until day 10 p.i., reaching parasitemia of ∼20%, and were cleared from mice at day 13 or 14 p.i., respectively. Mouse survival rate after injection of 10^4 or 10^5 *Pb*NK65-*hrf*Δ1 parasites was ∼90% and ∼70%, respectively. Notably, injection of 10^3 *Pb*NK65-*hrf*Δ1 parasites did not lead to parasite clearance or mouse survival. Infection with *Pb*NK65-*hrf*Δ2, a second clone, gave similar results (Fig. S1, F and G). We concluded that infection with parasites lacking HRF can self-resolve and that parasite clearance depends on the initial parasite load and/or time to threshold parasitemia. Further experiments were performed after injection of 10^5 *Pb*NK65-*hrf*Δ1 parasites.

To determine whether clearance of mutant parasites from the circulation could be caused by parasite retention in the spleen, the parasite load in this organ was measured by RT–quantitative PCR (RT-qPCR). After a dramatic retention of *Pb*NK65-*hrf*Δ1 parasites at day 6, parasites were no longer detected in the spleen at day 14 (Fig. 1 F), indicating that parasite clearance was not caused by retention in the spleen (Fig. 1 G). Moreover, macroscopic examination showed a more important splenomegaly at day 6 in *Pb*NK65-*hrf*Δ1–infected mice than in WT-infected mice, suggesting leukocyte infiltration in the mutant-infected spleen (Fig. 1, H–J).

IL-6, B cells, and T cells are critical for inhibition of *Pb*NK65-*hrf*Δ blood stage growth

Because HRF-deficient *Pb*ANKA sporozoites induce IL-6 production in the liver during preerythrocytic infection (Mathieu et al., 2015), we compared IL-6 levels in mouse spleens 6 d p.i with WT or *Pb*NK65-*hrf*Δ1 iRBCs. Levels of IL-6 mRNA and plasmatic IL-6 protein were higher in *Pb*NK65-*hrf*Δ1–infected mice than in WT-infected mice (Fig. 2, A and B). Given that recombinant *Pb*HRF protein is sufficient to down-regulate IL-6 expression in vivo (Mathieu et al., 2015), we tested whether clearance of mutant parasites was the consequence of elevated IL-6 by infecting IL-6^{KO} mice with mutant parasites. Mutant parasites developed normally in and eventually killed IL-6^{KO} mice (Fig. 2 C), phenocopying WT parasite behavior in WT mice (Fig. 1 E). We concluded that increased IL-6 accounts for mutant parasite clearance.

Immunostaining with leukocyte surface markers and anti–IL-6 antibodies of cells collected from the spleen at days 6 and 20 p.i. identified IL-6–producing cells as $Ly6G^+$ neutrophils at day 6 and both $Ly6G^+$ neutrophils and $CD11c^+$ DCs at day 20 (Fig. 2 D). Depletion of neutrophils (Fig. S2, A and B) or DCs (Fig. S2, C and D) in mutant-infected mice reduced splenomegaly (Fig. S2, E, F, H, and I) and cell counts (Fig. S2, G and J) compared with nondepleted mice, confirming the contribution of neutrophils and DCs in the splenomegaly caused by mutant infection.

IL-6 is known to regulate the acute phase of the immune response and major B and T cell functions (Kishimoto et al., 1992; Barton, 1997). To test whether B or T cells were involved in self-resolution of mutant infection, we infected mice lacking B cells (μS^{KO}) or T cells ($CD3^{KO}$) with WT or *Pb*NK65-*hrf*Δ1 parasites and monitored parasite development. B cell– or T cell–deficient mice were unable to control *Pb*NK65-*hrf*Δ1 blood stage multiplication and died with kinetics similar to WT mice infected with WT parasites (Fig. 2, E and F). The importance of T cells was confirmed by the normal multiplication of the mutant parasite upon mouse treatment of previously protected mice with anti-CD3 antibody (Fig. 2 G and Fig. S2 K). This indicated that B and T lymphocytes contributed to the clearance of mutant parasites.

*Pb*NK65-*hrf*Δ1 infection confers lasting protection in a species- and stage-transcendent manner

To determine whether resolved *Pb*NK65-*hrf*Δ1 parasite infection might confer protection against challenge, mutant-infected mice were challenged with 10^5 WT *Pb*NK65 iRBCs at days 20, 35, 68, 168, and 396 p.i. Mice were protected in all cases, displaying no detectable parasitemia at any time point, and survived for more than a year (Fig. 3 A). Mice challenged at days 20 and 23 p.i. with 10^5 RBCs infected with virulent *P. berghei* ANKA (Fig. 3 B) or *P. yoelii* YM (Fig. 3 C), respectively, were also protected and did not develop parasitemia. Next, we asked whether mutant-infected mice were also protected against a challenge with WT *Pb*NK65 sporozoites, the mosquito-transmitted parasite stage. Sporozoite challenge did not result in detectable blood stage infection (Fig. 3 D), and parasite genes were not detected in the blood by PCR (not depicted). To ascertain that protection indeed targeted preerythrocytic stages and not just emerging blood stage development, the livers of mice challenged with sporozoites were analyzed by RT-qPCR 40 h after sporozoite inoculation. As shown in Fig. 3 E, the parasite load was significantly lower in the liver of *Pb*NK65-*hrf*Δ1–protected mice compared with control mice. A similar protection was observed against heterologous *P. berghei* ANKA (Fig. 3 F) and *P. yoelii* YM (Fig. 3 G) sporozoite challenge. Therefore, infection with HRF-deficient blood stage *Pb*NK65 parasites induces long-lasting protection against malaria in a species- and stage-transcendent manner.

Mutant-induced immunity involves *Plasmodium*-specific IgG2c antibodies

To assess whether antibodies were involved in the anti–*Pb*NK65-*hrf*Δ1 response, anti–parasite-specific antibodies of various isotypes were quantified by ELISA in sera of mice 15 d p.i. with WT or *Pb*NK65-*hrf*Δ1 parasites. As shown in Fig. 4 A, mice infected with *Pb*NK65-*hrf*Δ1 produced higher levels of IgG antibodies than mice infected with WT parasites, essentially belonging to the IgG2c subclass and to a lesser extent to the IgG3 subclass (Fig. 4 A). Next, as shown by Western blot analysis of extracts from WT blood stages (Fig. 4 B), these antibodies recognized multiple *P. berghei* antigens in contrast to sera from WT *Pb*NK65–infected mice or from naive mice (Fig. 4 B). Interestingly, the IgG2c isotype, expressed in C57BL/6 mice in which the IgG2a heavy chain is deleted, is known to be the predominant isotype generated in antiviral antibody responses (Coutelier et al., 1987) and the most efficient IgG subclass for antipathogen FcR-mediated effector functions (Nimmerjahn and Ravetch, 2005). In most experimental mouse malaria models, parasite-specific antibodies have been shown to be predominantly skewed toward the IgG2c isotype (Ndungu et al., 2009).

Immunoprecipitation of *P. berghei* blood stage proteins with the IgG antibodies from mutant-infected mice and mass spectrometry of the immunoprecipitate revealed five *P. berghei* proteins targeted by the protective IgG response (Fig. S3, A and B). These included the vaccine candidates merozoite surface protein 1

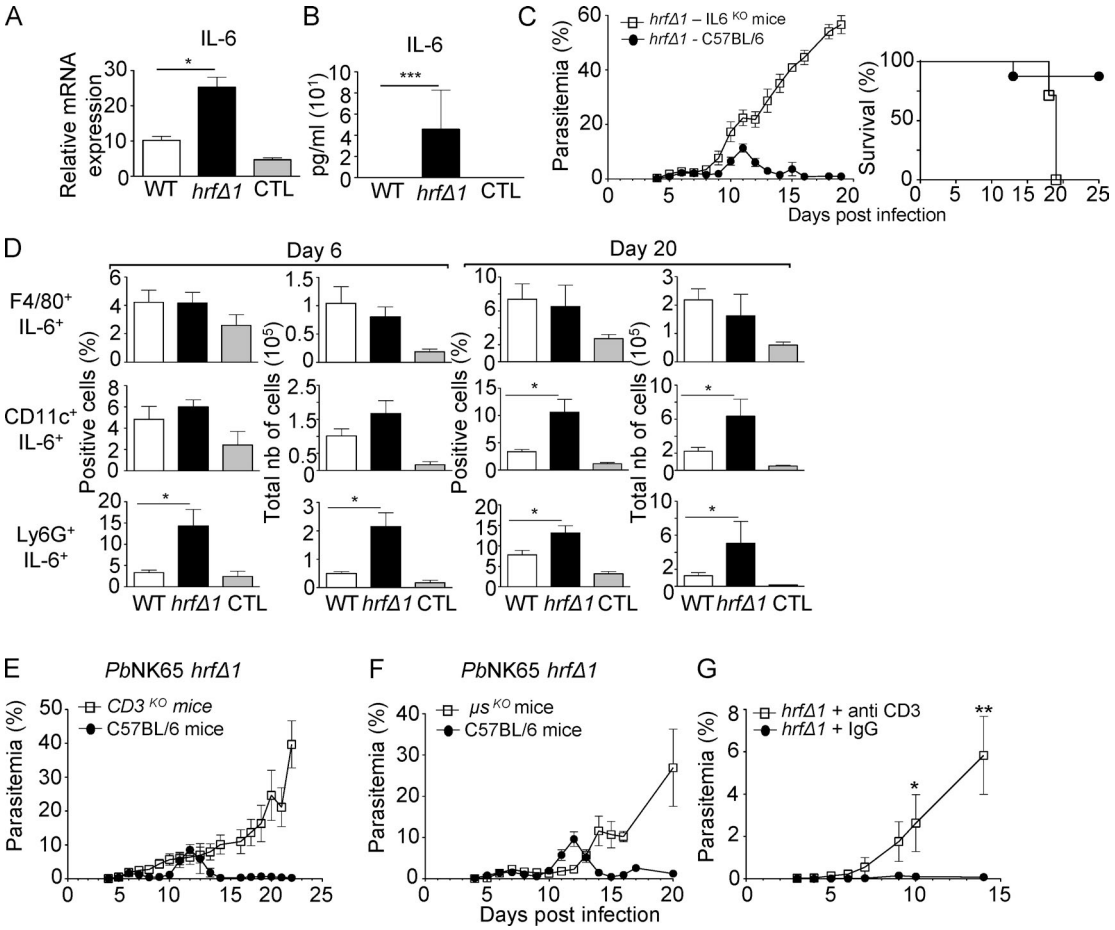

Figure 2. **IL-6 expression by neutrophils and DCs and T and B cells are essential for the clearance of *Pb*NK65-*hrf*Δ parasites.** (A and B) mRNA levels (RT-qPCR) normalized to HPRT of IL-6 in the spleen (A) and in the serum (ELISA; B) measured at day 6 p.i. from WT or *Pb*NK65-*hrf*Δ1–infected mice. Control (CTL): mRNA and sera from naive mice. (C) WT or IL-6^{KO} C57BL/6 mice were infected i.p. with 10^5 *Pb*NK65-*hrf*Δ1 iRBCs. Parasitemia and mouse survival (Kaplan-Meier survival plots: log-rank test; P = 0.0046) were followed over time. (D) Frequency and absolute numbers (nb) of IL-6–expressing splenic macrophages, DCs, and neutrophils at day 6 and day 20 p.i. from mice (five per group) infected with 10^5 WT or *Pb*NK65-*hrf*Δ1 iRBCs or from naive mice (CTL). (E and F) WT or T cell–deficient (E) or B cell–deficient (F) C57BL/6 mice were infected i.p. with 10^5 *Pb*NK65-*hrf*Δ1 iRBCs, and parasitemia was followed over time. (G) Protected mice were treated with IgG or with anti-CD3–depleting antibody 1 d prior to a challenge with WT parasites followed by two booster injections of anti-CD3 at days 1 and 3 after challenge. Error bars, SEM. Data are representative of four (A and B), three (C and E–G), and two (D) independent experiments with five to seven mice per group. *, 0.0028 < P < 0.046; **, P = 0.019; ***, P = 0.0097; Mann-Whitney test.

(MSP1), serine repeat antigen 1 (SERA1), and SERA2 (Bodescot et al., 2004; Putrianti et al., 2010; Alaro et al., 2013). As shown by immunoblots (Fig. S3 C) and ELISA (Fig. S3 D), only sera from protected mice recognized the recombinant MSP1-33 antigen.

Next, to test whether IgG antibodies may mediate parasite clearance via FcRγ-expressing cells, WT or FcRγ^{KO} C57BL/6 mice were infected with *Pb*NK65-*hrf*Δ1 parasites. As shown in Fig. 4 C, in contrast to WT mice, FcRγ^{KO} mice were unable to eliminate *Pb*NK65-*hrf*Δ1 parasites and phenocopied WT mice infected with WT parasites.

Antibodies and CD11b$^+$ cells from mutant-infected mice mediate protective immunity

Finally, to assess what immune effectors are important for protection, we performed passive transfer experiments. First, antibodies purified from protected mice were transferred to naive mice before challenge with WT *Pb*NK65 parasites. As shown in Fig. 4 D, parasitemia was lower in mice treated with IgG from protected mice than in normal IgG-treated mice, suggesting that antibodies alone provide partial but significant protective activity (Fig. 4 D).

Last, we asked whether CD11b$^+$ cells such as phagocytic leukocytes from *Pb*NK65-*hrf*Δ1–protected mice might be sufficient to protect naive mice from WT infection. WT C57BL/6 mice with adoptively transferred CD11b$^+$ cells from naive or *Pb*NK65-*hrf*Δ1–infected mice at day 15 p.i. were challenged with 10^5 WT parasites. As shown in Fig. 4 E, transfer of CD11b$^+$ cells from mutant-infected, but not naive, mice efficiently protected against infection. Collectively, these data suggest that

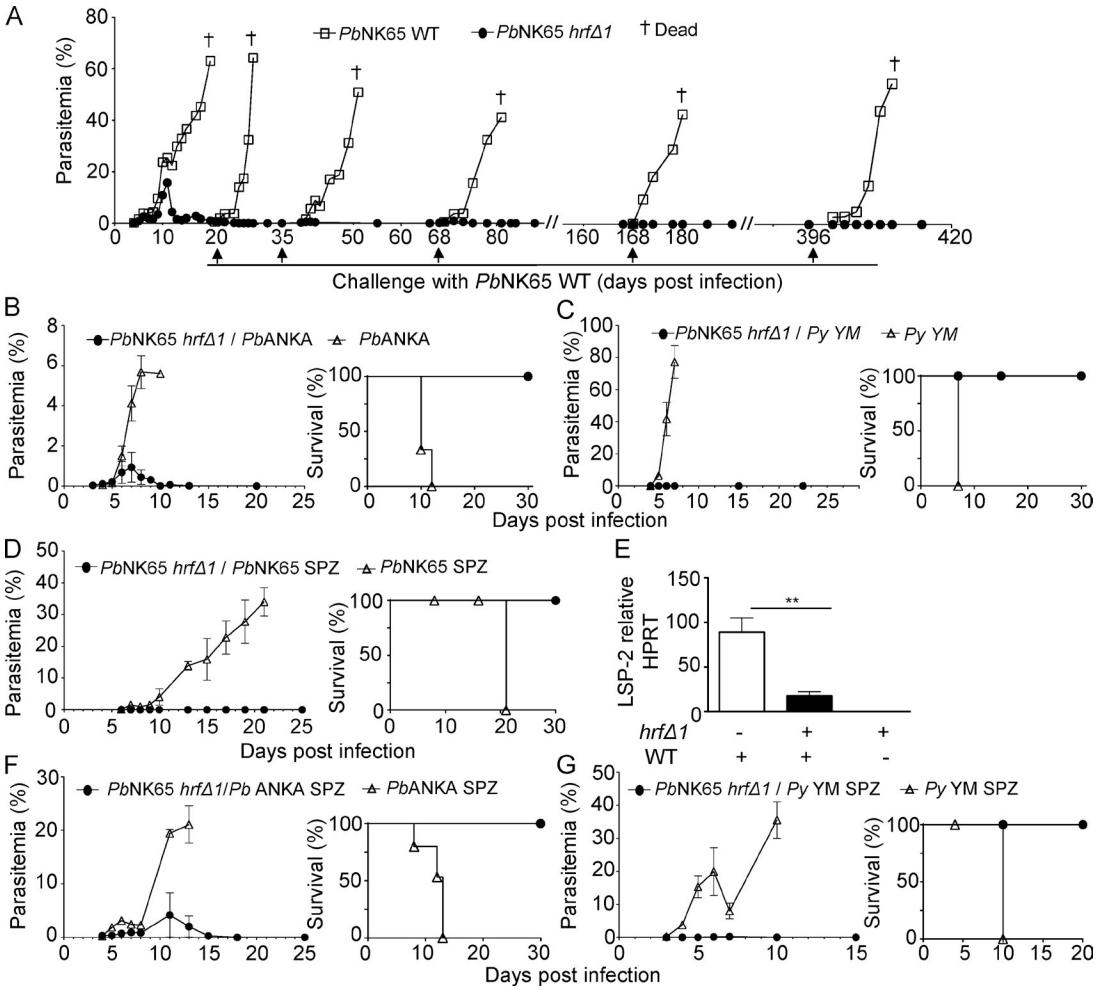

Figure 3. **Infection with HRF-deficient blood stage parasites ensures long-lasting cross-species and cross-stage protection.** (A) *Pb*NK65-*hrf*Δ1–protected mice were challenged with 10^5 WT *Pb*NK65 iRBCs at the indicated time points where control naive mice were also infected with 10^5 WT *Pb*NK65 iRBCs. (B–D) Parasitemia and survival were measured over time. Parasitemia and Kaplan-Meier survival plots of *Pb*NK65-*hrf*Δ1–protected mice challenged with 10^5 *Pb*ANKA (log-rank test; P = 0.0027; B) or *P. yoelii* YM (log-rank test; P = 0.0047; C) iRBCs at day 20 and day 23 p.i., respectively, or with 10^4 GFP-expressing WT *Pb*NK65 sporozoites (log-rank test; P = 0.0047) at day 36 p.i. (D). (E) Intrahepatic parasite development in experimental and control mice from D was assessed by RT-qPCR analysis of the liver stage–specific LSP-2 marker at 40 h p.i. of sporozoites. (F and G) *Pb*NK65-*hrf*Δ1–protected mice were challenged with 10^4 *Pb* ANKA (F) or *P. yoelii* YM (G) sporozoites at day 25 p.i., and parasitemia and survival (log-rank test; P = 0.0082) were determined over time. Naive mice infected on the same day with *Pb*ANKA (F) or with *P. yoelii* YM (G) sporozoites were used as controls. Error bars, SEM. Data are representative of two (A) and three (B–G) independent experiments with four to eight mice per group. **, P = 0.015; Mann-Whitney test. *Py*, *P. yoelii*; SPZ, sporozoites.

parasite antigen-specific antibodies and $Fc\gamma R^+$ $CD11b^+$ cells play an important part in mutant-induced protection.

This study shows that abortive blood stage infection leading to lasting protection can be achieved not just by impairing parasite intracellular growth, but also by enhancing protective immune responses. Indeed, lack of HRF and an increase in IL-6 do not affect parasite growth per se because *Pb*NK65-*hrfΔ* blood stages multiply normally in mice until day 10. Rather, IL-6, which is involved in B and T cell differentiation, boosts antiparasite adaptive responses that clear parasites. Like with previously reported blood stage GAPs that induce abortive infections, the protective response to *Pb*NK65-*hrfΔ* parasites is both solid, conferring cross-stage and cross-species immunity, and durable. We found that the protective response relies on the combination of antiparasite IgG2c antibodies and $Fc\gamma R^+$ $CD11b^+$ phagocytic cells, in particular neutrophils, which are sufficient for solid protection. Interestingly, the discovery of a B helper neutrophil population in the spleen that can act as professional helper cells for marginal zone B cells (Puga et al., 2012) highlights a neutrophil–B cell interplay that may be critical for B cell differentiation into antibody-producing plasma cells and may also contribute to inhibition of the well-known *Plasmodium* capacity to induce short-lived B cell memory (Wykes et al., 2005). Opsonic phagocytosis was also described as a protective mechanism induced by the plasmepsin-4–deficient mutant (Spaccapelo et al., 2010). Whether

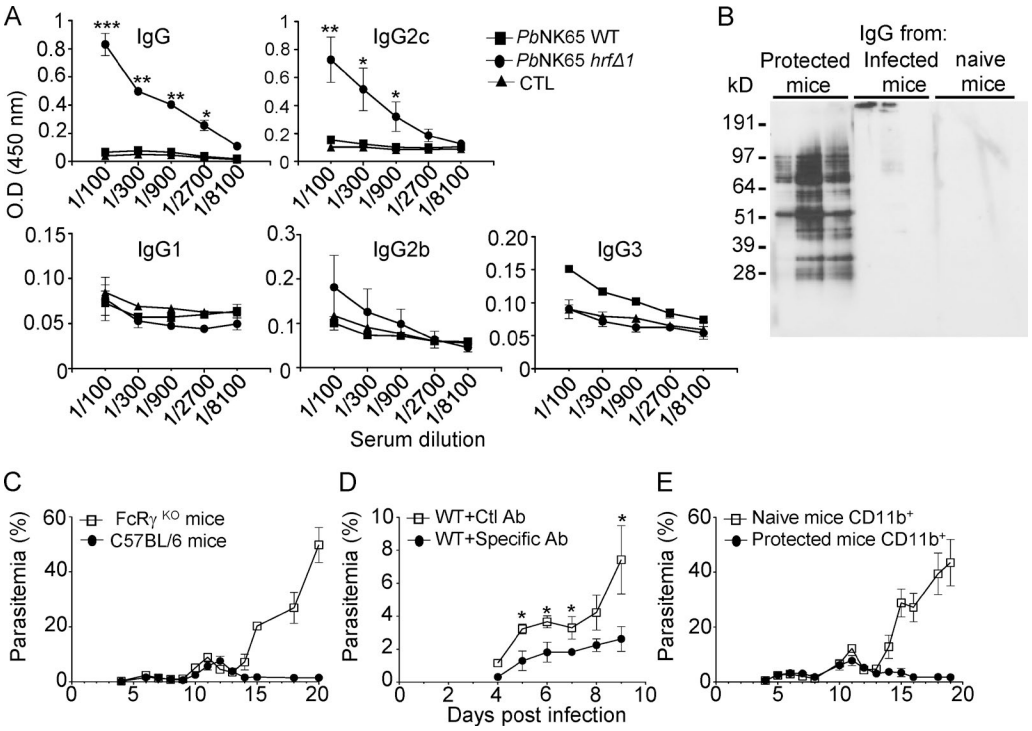

Figure 4. ***Pb*NK65-*hrf*Δ–induced immunity is T and B cell dependent and involves the secretion of *Plasmodium*-specific IgG2c antibodies.** (A) ELISA detection and quantification of antiparasite-specific antibodies of various isotypes in mouse sera at day 20 p.i. with WT or *Pb*NK65-*hrf*Δ1 parasites. Control (CTL): sera from naive mice. (B) Separated total protein extracts from WT *Pb*NK65 iRBCs were incubated with the IgG fraction from three independent mice infected with either *Pb*NK65-*hrf*Δ1 or WT parasites at day 20 p.i. or with normal mouse IgG. (C) C57BL/6 or FcRγ^{KO} mice were infected i.p. with 10^5 *Pb*NK65-*hrf*Δ1 iRBCs, and parasitemia was followed over time. (D) Purified IgG antibodies from *Pb*NK65-*hrf*Δ1–protected mice or from naive mice were injected i.p. 1 d before and 1 d after infection with 10^5 WT *Pb*NK65 iRBCs, and parasitemia was recorded over time. Ab, antibody; Ctl, control. (E) Sorted CD11b$^+$ cells from naive or *Pb*NK65-*hrf*Δ1–protected mice were transferred into WT C57BL/6 mice and immediately infected with 10^5 WT *Pb*NK65 iRBCs. Parasitemia was recorded over time. Error bars, SEM. Data are representative of three (A–D) and two (E) independent experiments with five to seven mice per group. *, 0.019 < P < 0.03; **, 0.0079 < P < 0.01; ***, P = 0.0002; Mann-Whitney test.

this represents the essential protective mechanism common to all self-resolving infections remains to be determined. Finally, although not formally demonstrated in our work, the contribution of parasite-specific CD8$^+$ cells to self-resolution cannot be precluded and awaits further investigation.

MATERIALS AND METHODS

Ethics statements. All experiments involving mice were conducted at Institut Pasteur, approved by the Direction Départementale des Services Vétérinaires' de Paris, France (permit number N° 75–066 issued on September 14, 2009), and performed in compliance with institutional guidelines and European regulations. A statement of compliance with the French government's ethical and animal experiment regulations was issued by the Ministère de l'Enseignement Supérieur et de la Recherche under the number 00218.01.

Rodents. 5–8-wk-old WT female C57BL/6J Rj and Swiss Webster (SW) mice were purchased from the Janvier laboratory. Transgenic T cell–deficient (CD3^{KO}), B cell–deficient (secretory μ chain [μs^{KO}]), Fcγ receptor–deficient (FcγR^{KO}), and IL-6^{KO} mice strains were provided by B. Ryffel (Institut Pasteur, Paris, France), J.M. Cavaillon (Institut Pasteur), P. Bruhns (Institut Pasteur), and L. Apetoh (Institut National de la Santé et de la Recherche Médicale U866, Dijon, France), respectively. CD11c-DTR (diphtheria toxin receptor)-GFP mice (Jung et al., 2002) have been used to explore the role of DCs in controlling parasite development. Transgenic mice have all been backcrossed 10 times on C57BL/6 mice from The Jackson Laboratory.

Parasites. Mice were inoculated with RBCs infected with either *P. berghei* (*Pb*) NK65 WT or mutant (*hrfΔ*) GFP-transgenic parasites. In a few control experiments, mice were infected with *P. yoelii* YM or *Pb* ANKA-GFP iRBCs, or with *Pb*NK65 or *Pb*ANKA GFP-transgenic sporozoites collected from salivary glands of infected *Anopheles stephensi*. Mosquitoes were provided by the CEPIA (Centre d'élevage, de production et d'infection des anopheles, Institut Pasteur).

Mouse infections and immunization with blood stages. Cryopreserved *P. berghei* parasites were passaged once through SW

mice before being used to infect experimental animals. Mice were infected with blood stages of either GFP-transgenic *Pb*NK65, *Pb*NK65-*hrf*Δ1, or *Pb*NK65-*hrf*Δ2 parasites by injecting 10^5, 10^4, or 10^3 iRBCs i.p. After injection, blood samples were taken daily from the tail, and parasitemia was assessed by flow cytometry. If mice did not develop parasites after challenge, they were recorded as completely protected.

Splenic index. Spleens from uninfected and infected mice were harvested at day 6 p.i. with WT or *Pb*NK65-*hrf*Δ1 parasites. The splenic index for each individual mouse was calculated as follows: spleen weight (mg)/body weight (mg) × 100.

Sporozoite development in HepG2 cells. HepG2 cells (2–3 × 10^4/well) were plated in 8-well chamber slides (Lab-Tek) and cultured overnight in DMEM + GlutaMAX-I media (Gibco) supplemented with 10% heat-inactivated FBS (Gibco) at 37°C in the presence of 5% CO_2. WT or mutant purified *P. berghei* salivary gland sporozoites were used for HepG2 infection at a ratio of 1:1 (parasite/cells) for 36 h at 37°C with 5% CO_2 in the presence of penicillin–streptomycin–neomycin solution (Sigma-Aldrich). *Pb*HRF was detected by immunofluorescence staining as described in the next paragraph.

Immunofluorescence assays for the intracellular detection of HRF. Fixation and permeabilization of sporozoites, infected HepG2 cells, iRBCs, and purified gametocytes were performed using 4% paraformaldehyde and 0.1% Triton X-100 and blocked with 1–3% gelatin from porcine skin (Sigma-Aldrich). Thereafter, cells were incubated with specific rabbit anti-HRF antibodies (diluted 1:500; Mathieu et al., 2015) and then incubated with Alexa Fluor 568–conjugated secondary antibodies (diluted 1:500; Thermo Fisher Scientific) and 0.02 mg/ml DAPI for nuclear staining. The expression of *Pb*HRF was detected using a fluorescence microscope (AxioVert 200; ZEISS).

Preparation of total RNA and RT-qPCR analysis of mRNA. The spleens and livers of C57BL/6J mice infected with WT or *Pb*NK65-*hrf*Δ1 parasites were surgically removed 40 h p.i. or at day 2, 4, 6, 8, 10, 12, 14, and 20 p.i., respectively. Total RNAs were extracted from the spleen as well as from liver samples using the guanidinium-thiocyanate-phenol-chloroform method (all from Invitrogen). RNA was thereafter reverse transcribed by PCR (temperature profile: 65°C for 5 min, 42°C for 50 min, and 70°C for 15 min) using 100 U of SuperScript II reverse transcriptase (Invitrogen), 40 U RNase inhibitor, and 2 µM oligo(dT) 18S rRNA primer (Eurofins MWG Operon) per sample. The expression levels of diverse transcripts were analyzed by real-time RT-qPCR using Power SYBR green PCR master mix (Applied Biosystems) and various primer sets (Table S1). All reactions were performed in a real-time PCR machine (temperature profile: 50°C for 2 min, 95°C for 10 min, 40 cycles of 15 s at 95°C, and 60°C for 1 min; ABI PRISM 7000 Sequence Detection System; Applied Biosystems). The relative abundance of parasite and cytokine rRNA in the spleen was calculated using the ΔC_t method and expressed as $2^{-\Delta C_t}$. The mouse hypoxanthine phosphoribosyltransferase (HPRT) gene was used as an internal control for the variation in input RNA amounts. A no-template control was included to ensure that there was no cross-contamination during sample preparation.

Flow cytometry analysis of spleen leukocytes. Spleens were mechanically disrupted in 2 ml PBS, and cells were filtered through a 70-mm strainer (BD). Erythrocytes were lysed using Gey's solution for 5 min on ice and washed twice in PBS. Single-cell suspensions were stained for FACS analysis according to standard protocols in cold PBS containing 2% FCS and 0.01% sodium azide (FACS buffer) with the following antibodies: PE-labeled anti-CD4, PE-Cy5–labeled anti-CD45, allo phyco cyanine (APC)–labeled anti-CD8, FITC-labeled anti-CD11b, APC-labeled anti-CD11c, APC-labeled anti-Ly6G, PE-Cy5–labeled anti-F4/80, and PE-labeled anti–IL-6 antibodies (all antibodies from BD). A total of 5 × 10^5 living cells were analyzed using a four-color flow cytometer (FAC SCalibur; BD) and ProCellQuest software (BD).

In vivo cell depletion. For neutrophil depletion, C57BL/6 mice were injected with 500 µg of a rat anti–mouse neutrophil (clone NIMP-R14) provided by G. Milon (Institut Pasteur) at day 2 and day 4 p.i. with *Pb*NK65-*hrf*Δ1. For systemic DC depletion, CD11c-DTR-GFP transgenic mice were injected i.p. with 5.2 ng/g body weight diphtheria toxin (Sigma-Aldrich) in PBS at days 2 and 4 p.i. with *Pb*NK65-*hrf*Δ1. To determine whether CD3 plays a role in the antiparasitic memory response developed by protected mice, cell-specific depletion experiments were performed. C57BL/6J Rj–protected mice were injected i.p. with 20 µg anti-CD3 (clone 145-2C11) Armenian hamster IgG (eBioscience) 24 h before the infection with *Pb*NK65 WT and 48 h p.i. The cell depletion was followed and confirmed by flow cytometry. Before the infection and every day p.i., 10 µl of blood was collected from the tip of the mouse tail and analyzed to confirm neutrophil, DC, and CD3 cell depletion by FACS analysis.

Detection of specific IgG antibodies and IL-6 cytokine in the serum of infected mice. To detect parasite-specific antibodies, protein extracts from blood stages obtained by saponin lysis (0.1%) of parasite pellets were sonicated in lysis buffer (10 mM Tris, pH 7.4, 150 mM NaCl, 0.02% NaN_3, 20 mM $MgCl_2$, 1% Triton X-100, and complex protease inhibitors) and centrifuged (10,000 *g* for 30 min at 4°C). The total amount of proteins in the supernatant was measured using a Bio-Rad Laboratories protein assay. 96-well plates (Nunc-immuno plate; Thermo Fisher Scientific) were coated with 2 µg/ml *Pb*NK65 WT protein extracts in carbonate buffer, pH 9.6, for 2 h at 37°C and then saturated with 1% (wt/vol) BSA (Sigma-Aldrich). Serum samples were assayed using serial dilutions and incubated for 2 h at 37°C. Specific binding was detected

using HRP-conjugated goat anti–mouse secondary antibody (diluted 1:2,000; Cell Signaling Technology) followed by the addition of *o*-phenylenediamine dihydrochloride substrate (Sigma-Aldrich). HCl 1N was used to block the reaction. The optical density was read at 490–630 nm. Each sample was tested against nonimmune serum and PBS as background controls. Amounts of IL-6 in the serum were analyzed following the instructions provided by the ELISA kit supplier (BD).

Western blotting. 20 µg *Pb*NK65 WT protein extract from asexual blood stages were separated by SDS-PAGE (4–12% Bis-Tris gels; BOLT mini gel system; Thermo Fisher Scientific) and transferred onto a polyvinylidene fluoride membrane (iBLOT system; Thermo Fisher Scientific). Sera from uninfected, WT, or *Pb*NK65-*hrf*Δ1 mice were added (1:1,000 dilution) and incubated overnight at 4°C. After washing the membrane with PBS + Tween 20 (Sigma-Aldrich), polyclonal anti–mouse IgGs (1:20,000; P0260; Dako) were added, and specific bands were visualized with the SuperSignal West Pico kit (Thermo Fisher Scientific) according to the manufacturer's instructions.

Adoptive transfer of IgG-specific antibodies and CD11b-positive cells. C57BL/6J mice were infected with either WT or *Pb*NK65-*hrf*Δ1 parasites as described in the previous paragraph. Specific IgGs and $CD11b^+$ cells were obtained from challenged protected mice at day 15 p.i. Immune sera were collected, and the IgG fraction was purified on an immunoabsorbent protein G–Sepharose column (BioVision). 100 µg IgGs was transferred i.p. into naive mice 24 h before WT *Pb*NK65 iRBC infection. Mice were then given 100 µg of antibody on days 3 and 6 p.i. Single-cell suspension of $CD11b^+$ cells was obtained from naive or *Pb*NK65-*hrf*Δ1–infected mice by FACs sorting of spleen and bone marrow cells stained with FITC-labeled anti-CD11b. Each mouse received intravenous injections of 2.5×10^6 $CD11b^+$ cells 1 h after WT *Pb*NK65 iRBC infection.

Generation and cloning of *Pb*NK65-*hrf*Δ parasites. For construction of the targeting vector for *pbhrf* disruption (*PbHRF*; plasmid provided by P. Smooker and K. Taylor, RMIT University, Bundoora, Australia), DNA fragments corresponding to the 5′ untranslated (UTR) and 3′UTR regions of the *pbhrf* gene were amplified by PCR using *P. berghei* NK65 genomic DNA (gDNA) as a template. These primers (Table S2) were tailed with restriction sites for ApaI, PstI, KpnI, and EcoRI to facilitate cloning into either side of the *hDHFR* cassette (de Koning-Ward et al., 2000) in pUC18 backbone. The targeting construct was integrated into the *pbhrf* gene locus by double crossover recombination, resulting in the disruption of *pbhrf* and conferring WR99210 or pyrimethamine resistance. Transfection into a GFP-*Pb*NK65 parasite strain and selection of recombinant parasite clones were performed as previously described (Janse et al., 2006). In brief, after overnight culture (37°C with 10% O_2 and 5% CO_2 at 90 rpm) of the blood of infected animals, mature schizonts were purified using a Nycodenz gradient and collected at room temperature. The electroporation mix was composed of 10^7–10^8 merozoites resuspended in 50 µl and 100 µl of human T cell Nucleofector solution (Amaxa) and 5 µl DNA (containing 5 µg of digested DNA in water). Parasites were electroporated using the U33 program of the Nucleofector electroporator (Amaxa) and immediately resuspended in PBS and injected intravenously into 3-wk-old female SW mice. Recipient mice were treated with 0.07 mg/ml pyrimethamine in drinking water or with 6 mg/kg WR99210 by subcutaneous injections, starting 24 h after electroporation. At day 6 after electroporation, the emerging parasite population was collected, gDNA was extracted, and genomic integration of the *hDHFR* cassette (within the *pbhrf* locus of GFP-*Pb*NK65 transfectants) was confirmed using specific PCR primers: (a) Apa-5′UTR *Pb*HRF-F and EcoRI-3′UTR *PbHRF*-R, (b) *HRF*5′-F and *hDHFR*5′-R, and (c) *HRF*3′-R and h*DHFR*3′-F. The first pair of primers (Apa-5′UTR *PbHRF*-F and EcoRI-3′UTR *PbHRF*-R) amplified gDNA encompassed by the ApaI and EcoRI restriction sites and inclusive of the *pbhrf* 5′ and 3′UTRs. A PCR product of 2,681 bp was indicative of *hrf*Δ, whereas a PCR product of 1,760 bp denoted a WT genotype. The second pair of primers (*HRF*5′-F and h*DHFR*5′-R) amplified DNA ouside the *hDHFR* insert (inclusive of the 5′UTR *PbHRF*) and within the 5′ region of the *hDHFR* cassette, respectively. A PCR product of 700 bp indicated a *hrf*Δ clone, whereas absence of a band denoted a WT genotype. The third pair of primers (h*DHFR*3′-F and *HRF*3′-R) amplified gDNA within the 3′ region of the *hDHFR* cassette and outside the *hDHFR* insert (inclusive of the 3′UTR *pbhrf*), respectively. A PCR product of 1,100 bp indicated a *hrf*Δ clone, whereas absence of a band indicated a WT genotype.

Statistical analysis. All data were analyzed using Prism 5.0 software (GraphPad Software). Unpaired data between two groups at a specific time point were analyzed by a Mann-Whitney test for nonparametric analysis when data did not fit a Gaussian distribution. A p-value <0.05 was considered to be statistically significant. All experiments were replicated several times as indicated in the figure legends.

Southern blotting. gDNA was obtained as follows: parasite pellets obtained by saponin lysis of iRBCs were resuspended in PBS and treated with 150 µg/ml proteinase K and 2% SDS at 55°C for 20 min. The DNA was isolated from the parasite pellet using the DNeasy blood and tissue kit (QIAGEN). The DNA was digested with EcoRV and probed with an *hrf* probe.

Mass spectrometry analysis, database search, protein identification, and statistical analysis. After the immunoprecipitation, proteins were solubilized in denaturation buffer (10 mM Tris, pH 8, and 8 M urea). Proteins were reduced, alkylated, and digested with trypsin. Tryptic peptides were analyzed by

nano LC-MS/MS (liquid chromatography coupled with tandem mass spectrometry) using a chromatograph (EASY-nLC 1000; Thermo Fisher Scientific) coupled to a mass spectrometer (Q Exactive Orbitrap). About 1 µg of each sample (dissolved in 0.1% formic acid [FA]) was loaded at 250 nl/min on a homemade C18 50-cm capillary column picotip silica emitter tip (75-µm diameter filled with 1.9 µm Reprosil-Pur Basic C18-HD resin [Dr. Maisch GmbH]) equilibrated in solvent A (0.1% FA). The peptides were eluted using a two-slopes gradient of solvent B (0.1% FA in acetonitrile) from 2–30% in 90 min and from 30–80% in 60 min at a 250-nl/min flow rate (total length of the chromatographic run was 180 min). The mass spectrometer (Q Exactive Orbitrap; Thermo Fisher Scientific) was operated in data-dependent acquisition mode with XCalibur software (version 2.2; Thermo Fisher Scientific). Survey scan MSs were acquired in the Orbitrap on the 300–1,800-m/z range with the resolution set to a value of 70,000 at m/z = 400 in profile mode (automatic gain control target at 1E6). The 20 most intense ions per survey scan were selected for higher energy collisional dissociation fragmentation (NCE 28), and the resulting fragments were analyzed in the mass spectrometer at 17,500 resolution (m/z of 400). Isolation of parent ion was fixed at 2.5 m/z, and the underfill ratio was fixed at 0.1%. Dynamic exclusion was used within 20 s. Each sample was prepared in triplicate.

Data were searched using MaxQuant (version 1.4.1.2; with the Andromeda search engine) against the Plasmodium_berghei database (22,006 entries). The following search parameters were applied. Carbamidomethylation of cysteines was set as a fixed modification. Oxidation of methionine and protein N-terminal acetylation were set as variable modifications. The mass tolerances in MS and MS/MS were set to 10 parts per million for each, respectively. Two peptides were required for protein identification and quantitation. Peptides and proteins identified with a false discovery rate <0.01% were considered as valid identification. Statistical analysis of the data was performed using Perseus, R package, MSstat, and internal tools. Two sample Student's *t* tests were used to identify significantly regulated proteins between two groups. The results were visualized on volcano plots.

Immunoprecipitation. Immunoprecipitation of *Pb* proteins from parasite extracts was performed using the Pierc Direct immunoprecipitation kit (Thermo Fisher Scientific). Before immunoprecipitation, 10 µg of purified IgG antibodies from the serum of protected, infected, and naive mice was directly immobilized onto an agarose support (AminoLink Plus Resin) using a short coupling protocol. 500–700 µg of parasite extracts was incubated with the immobilized antibody to form the immune complex with gentle end-over-end mixing overnight at 4°C. To remove nonbound material, beads were washed three times with wash buffer, and a low pH elution buffer was used to dissociate the bound antigen from the antibody. Immunoprecipitated proteins were then used for mass spectrometry analysis.

Online supplemental material. Fig. S1 shows disruption of the *pbhrf* gene in *Pb*NK65 parasites. Fig. S2 shows assessment of leukocyte depletion and the role of neutrophils and DCs in the occurrence of splenomegaly. Fig. S3 shows identification of immune sera–derived immunoprecipitated proteins. Table S1 contains a list of oligonucleotides used for RT-qPCR analyses. Table S2 contains a list of oligonucleotides used for PCR of WT and recombinant parasites. Online supplemental material is available at http://www.jem.org/cgi/content/full/jem.20151976/DC1.

ACKNOWLEDGMENTS

We thank Peter Smooker and Kim Taylor for providing *P. berghei* HRF plasmid the CEP IA for providing *A. stephensi*, Shruthi Vembar for her thorough revision of the manuscript, and Veronique Hourdel for her technical assistance for mass spectrometry.

This work was funded by an Institut Pasteur grant to S. Mécheri. C. Demarta-Gatsi is supported by a predoctoral fellowship from the Helmut Horten Foundation.

The authors declare no competing financial interests.

Submitted: 18 December 2015
Accepted: 26 May 2016

REFERENCES

Alaro, J.R., A. Partridge, K. Miura, A. Diouf, A.M. Lopez, E. Angov, C.A. Long, and J.M. Burns Jr. 2013. A chimeric *Plasmodium falciparum* merozoite surface protein vaccine induces high titers of parasite growth inhibitory antibodies. *Infect. Immun.* 81:3843–3854. http://dx.doi.org/10.1128/IAI.00522-13

Aly, A.S., M.J. Downie, C.B. Mamoun, and S.H. Kappe. 2010. Subpatent infection with nucleoside transporter 1-deficient *Plasmodium* blood stage parasites confers sterile protection against lethal malaria in mice. *Cell. Microbiol.* 12:930–938. http://dx.doi.org/10.1111/j.1462-5822.2010.01441.x

Barton, B.E. 1997. IL-6: insights into novel biological activities. *Clin. Immunol. Immunopathol.* 85:16–20. http://dx.doi.org/10.1006/clin.1997.4420

Beghdadi, W., A. Porcherie, B.S. Schneider, D. Dubayle, R. Peronet, M. Huerre, T. Watanabe, H. Ohtsu, J. Louis, and S. Mécheri. 2008. Inhibition of histamine-mediated signaling confers significant protection against severe malaria in mouse models of disease. *J. Exp. Med.* 205:395–408. http://dx.doi.org/10.1084/jem.20071548

Bhisutthibhan, J., M.A. Philbert, H. Fujioka, M. Aikawa, and S.R. Meshnick. 1999. The *Plasmodium falciparum* translationally controlled tumor protein: subcellular localization and calcium binding. *Eur. J. Cell Biol.* 78:665–670. http://dx.doi.org/10.1016/S0171-9335(99)80052-1

Bodescot, M., O. Silvie, A. Siau, P. Refour, P. Pino, J.F. Franetich, L. Hannoun, R. Sauerwein, and D. Mazier. 2004. Transcription status of vaccine candidate genes of *Plasmodium falciparum* during the hepatic phase of its life cycle. *Parasitol. Res.* 92:449–452. http://dx.doi.org/10.1007/s00436-003-1061-9

Coutelier, J.P., J.T. van der Logt, F.W. Heessen, G. Warnier, and J. Van Snick. 1987. IgG2a restriction of murine antibodies elicited by viral infections. *J. Exp. Med.* 165:64–69. http://dx.doi.org/10.1084/jem.165.1.64

de Koning-Ward, T.F., D.A. Fidock, V. Thathy, R. Menard, R.M. van Spaendonk, A.P. Waters, and C.J. Janse. 2000. The selectable marker human dihydrofolate reductase enables sequential genetic manipulation of the *Plasmodium berghei* genome. *Mol. Biochem. Parasitol.* 106:199–212. http://dx.doi.org/10.1016/S0166-6851(99)00189-9

Janse, C.J., J. Ramesar, and A.P. Waters. 2006. High-efficiency transfection and drug selection of genetically transformed blood stages of the rodent malaria parasite *Plasmodium berghei*. *Nat. Protoc.* 1:346–356. http://dx.doi.org/10.1038/nprot.2006.53

Jung, S., D. Unutmaz, P. Wong, G. Sano, K. De los Santos, T. Sparwasser, S. Wu, S. Vuthoori, K. Ko, F. Zavala, et al. 2002. In vivo depletion of $CD11c^+$ dendritic cells abrogates priming of $CD8^+$ T cells by exogenous cell-associated antigens. *Immunity.* 17:211–220. http://dx.doi.org/10.1016/S1074-7613(02)00365-5

Kishimoto, T., S. Akira, and T. Taga. 1992. Interleukin-6 and its receptor: a paradigm for cytokines. *Science.* 258:593–597. http://dx.doi.org/10.1126/science.1411569

Mathieu, C., C. Demarta-Gatsi, A. Porcherie, S. Brega, S. Thiberge, K. Ronce, L. Smith, R. Peronet, R. Amino, R. Ménard, and S. Mécheri. 2015. *Plasmodium berghei* histamine-releasing factor favours liver-stage development via inhibition of IL-6 production and associates with a severe outcome of disease. *Cell. Microbiol.* 17:542–558. http://dx.doi.org/10.1111/cmi.12382

Miyagami, T., I. Igarshi, and M. Suzuki. 1987. Plasmodium berghei: long lasting immunity induced by a permanent attenuated mutant. *Zentralbl. Bakteriol. Mikrobiol. Hyg. [A].* 264:502–512.

Ndungu, F.M., E.T. Cadman, J. Coulcher, E. Nduati, E. Couper, D.W. Macdonald, D. Ng, and J. Langhorne. 2009. Functional memory B cells and long-lived plasma cells are generated after a single *Plasmodium chabaudi* infection in mice. *PLoS Pathog.* 5:e1000690. http://dx.doi.org/10.1371/journal.ppat.1000690

Nimmerjahn, F., and J.V. Ravetch. 2005. Divergent immunoglobulin g subclass activity through selective Fc receptor binding. *Science.* 310:1510–1512. http://dx.doi.org/10.1126/science.1118948

Pied, S., L. Rénia, A. Nüssler, F. Miltgen, and D. Mazier. 1991. Inhibitory activity of IL-6 on malaria hepatic stages. *Parasite Immunol.* 13:211–217. http://dx.doi.org/10.1111/j.1365-3024.1991.tb00276.x

Pombo, D.J., G. Lawrence, C. Hirunpetcharat, C. Rzepczyk, M. Bryden, N. Cloonan, K. Anderson, Y. Mahakunkijcharoen, L.B. Martin, D. Wilson, et al. 2002. Immunity to malaria after administration of ultra-low doses of red cells infected with *Plasmodium falciparum*. *Lancet.* 360:610–617. http://dx.doi.org/10.1016/S0140-6736(02)09784-2

Puga, I., M. Cols, C.M. Barra, B. He, L. Cassis, M. Gentile, L. Comerma, A. Chorny, M. Shan, W. Xu, et al. 2012. B cell-helper neutrophils stimulate the diversification and production of immunoglobulin in the marginal zone of the spleen. *Nat. Immunol.* 13:170–180. http://dx.doi.org/10.1038/ni.2194

Putrianti, E.D., A. Schmidt-Christensen, I. Arnold, V.T. Heussler, K. Matuschewski, and O. Silvie. 2010. The *Plasmodium* serine-type SERA proteases display distinct expression patterns and non-essential in vivo roles during life cycle progression of the malaria parasite. *Cell. Microbiol.* 12:725–739. http://dx.doi.org/10.1111/j.1462-5822.2009.01419.x

Spaccapelo, R., C.J. Janse, S. Caterbi, B. Franke-Fayard, J.A. Bonilla, L.M. Syphard, M. Di Cristina, T. Dottorini, A. Savarino, A. Cassone, et al. 2010. Plasmepsin 4-deficient *Plasmodium berghei* are virulence attenuated and induce protective immunity against experimental malaria. *Am. J. Pathol.* 176:205–217. http://dx.doi.org/10.2353/ajpath.2010.090504

Spaccapelo, R., E. Aime, S. Caterbi, P. Arcidiacono, B. Capuccini, M. Di Cristina, T. Dottorini, M. Rende, F. Bistoni, and A. Crisanti. 2011. Disruption of plasmepsin-4 and merozoites surface protein-7 genes in *Plasmodium berghei* induces combined virulence-attenuated phenotype. *Sci. Rep.* 1:39. http://dx.doi.org/10.1038/srep00039

Ting, L.M., M. Gissot, A. Coppi, P. Sinnis, and K. Kim. 2008. Attenuated *Plasmodium yoelii* lacking purine nucleoside phosphorylase confer protective immunity. *Nat. Med.* 14:954–958. http://dx.doi.org/10.1038/nm.1867

Waki, S., J. Tamura, M. Imanaka, S. Ishikawa, and M. Suzuki. 1982. *Plasmodium berghei*: isolation and maintenance of an irradiation attenuated strain in the nude mouse. *Exp. Parasitol.* 53:335–340. http://dx.doi.org/10.1016/0014-4894(82)90076-5

Wykes, M.N., Y.H. Zhou, X.Q. Liu, and M.F. Good. 2005. *Plasmodium yoelii* can ablate vaccine-induced long-term protection in mice. *J. Immunol.* 175:2510–2516. http://dx.doi.org/10.4049/jimmunol.175.4.2510